Single-neuron responses and neuronal decisions in a vernier task

Ying Zhang and R. Clay Reid*

Department of Neurobiology, Harvard Medical School, 220 Longwood Avenue, Boston, MA 02115

Communicated by David H. Hubel, Harvard Medical School, Boston, MA, December 31, 2004 (received for review June 10, 2004)

Vernier acuity is a measure of the smallest horizontal offset between two vertical lines that can be behaviorally discriminated. To examine the link between the neuronal responses in a retinotopic mosaic and vernier acuity, we recorded the responses of single cells in cat lateral geniculate nucleus to a vertical bar stimulus that was stepped in small increments through the receptive fields of cells. Based on the single-trial responses evoked by stimuli at different positions, we calculated the spatial resolution that could be achieved. If the stimulus could fall anywhere in their receptive fields, single neurons had spatial resolutions two times worse than previously reported vernier thresholds. Given the known coverage factor in a cat retina, we developed a two-stage decision model to examine how the responses of neurons in a retinotopic mosaic could be processed to achieve vernier acuity. In order for psychophysical thresholds to be accounted for by the responses of a single cell, the stimulus must fall in the quarter of the receptive field that provides the most information about stimulus position. Alternatively, both the absolute psychophysical threshold for vernier acuity and its dependence on stimulus length can be realized by pooling the responses of a few neurons, all located on one side of the bar stimulus.

hyperacuity | retinal mosaic | vision | sensory perception

The link between the responses of single cells in the nervous system and sensory perception remains one of the most important and puzzling problems in neuroscience (1). In a great many cases, the relationship between the two follows a simple principle: the sensitivity of single units is comparable with psychophysical sensitivity (2–8). This principle asserts that psychophysical acuity can be accomplished by the response from a single neuron, but it does not exclude the integration of multiple neurons. Only in very rare cases has the sensitivity of single units been documented as being worse than psychophysical sensitivity (9). Under such circumstances, the integration of information from more than a single neuron is a prerequisite demanded by the experimental data.

Vernier acuity, the psychophysical threshold for discriminating a spatial offset between two vertical lines, is one of the most sensitive measures of visual discrimination (10, 11). The vernier acuity of human subjects can be as small as 6 seconds of arc (hereafter, sec arc) (10). Vernier acuity is considered hyperacuity because it is five times finer than resolution acuity (≈30 sec arc, roughly the same as the foveal cone spacing; ref. 12). A similar relative level of hyperacuity in vernier tasks has been measured behaviorally in both cats (≈1–2 min arc) (13, 14) and monkeys (≈10 sec arc) (15, 16). Because of the high level of psychophysical vernier acuity compared with the size of the smallest receptive fields (RFs), it is likely that information must be integrated from multiple neurons to achieve perceptual discriminations.

Vernier acuity is measured by a vernier task, a two-alternative, forced-choice discrimination task (10, 11). When a vernier task is performed, the eyes of the experimental subject cannot be controlled to an accuracy as fine as the smallest RFs. The vernier stimulus might therefore fall at any position within the RF of a given neuron in the retina or lateral geniculate nucleus (LGN). To mimic psychophysical experiments, we examined the ability of LGN cells to discriminate between closely spaced stimuli throughout their RFs, under conditions in which the eye position could be controlled with great precision. Although it has been shown that a single cell can exceed behavioral performance when stimuli fall at particular positions within the RF, the capacity of a single cell to make fine discriminations throughout its entire RF has not been explicitly studied (17–19).

To examine the ability of single neurons to discriminate between two closely spaced stimuli throughout their RFs, we recorded the responses of neurons in cat LGN, where RF size is comparable with those of retinal ganglion cells and the stability of the recordings is superior (20). Taking advantage of the highly organized retinotopic map in the LGN and the large body of anatomical and physiological knowledge concerning the cat visual system, we then developed a two-stage neuronal decision model and explored how information might be integrated from the collective responses of multiple neurons. We wanted to know how the responses of a retinotopic mosaic might be processed to provide the minimal amount of information required to underlie a vernier decision.

Materials and Methods

Preparation and Electrophysiology. Our procedure for recording from anesthetized and paralyzed cats is given in refs. 21 and 22. With an initial dosage of ketamine (10 mg/kg i.m.), the cats were anesthetized by pentothal (continuous 4 mg/kg per hr with 20 mg/kg supplement as needed i.v.) and paralyzed by vecuronium bromide (0.2–0.3 mg/kg per hr i.v.). The animal's temperature, expired CO_2 level, electrocardiogram, and electroencephalogram were continuously monitored throughout the experiments. The action potentials of single LGN neurons were recorded with plastic-coated tungsten electrodes (A-M Systems, Everett, WA); the waveforms were collected at 0.1-ms resolution with the DISCOVERY data acquisition program (DataWave Technologies, Longmont, CO). Eyes were refracted by back projecting retinal vessels onto a tangent screen placed 114 cm in front of the animal. To minimize the effect of possible eye movements, the sclera was sutured and glued to a metal ring that was mounted on the stereotaxic frame. In some experiments, a contact lens with a 3-mm artificial pupil was used to reduce light scatter, but the results were qualitatively similar to those obtained with a clear lens.

Visual Stimuli and Receptive Fields. Receptive fields were first characterized by spatiotemporal white noise stimuli that consisted of a 16 × 16 grid of squares that were alternated between black and white according to a pseudorandom temporal signal (22). All stimuli were presented on a computer monitor with a refresh rate of 128 Hz and mean luminance of ≈50 cd/m^2. RF plots (temporal weighting functions) were calculated by reverse correlation (23). A contour plot of the RF measured at the

Abbreviations: LGN, lateral geniculate nucleus; RF, receptive field.

*To whom correspondence should be addressed. E-mail: clay_reid@hms.harvard.edu.

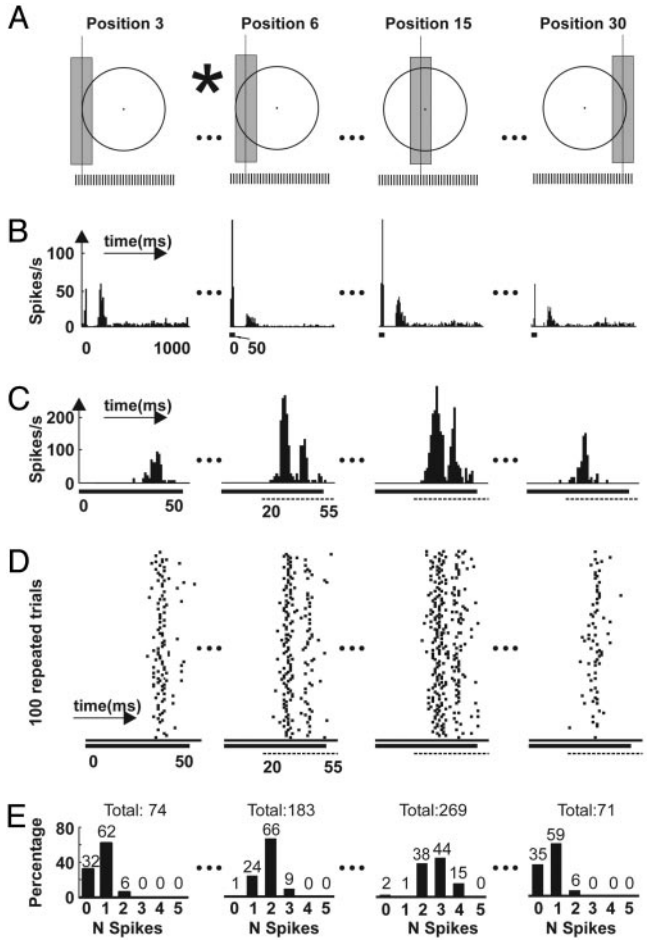

Fig. 1. Reponses of an off-center LGN cell to a 50-ms flash at multiple positions. (*A*) Schematic diagram of the bar stimulus and RF center of an LGN cell (diameter: 2.05°). The dark stimulus (0.45° wide, 100% contrast) was flashed at 33 positions (S_1–S_{33}), with 0.057° spacing. Four representative positions, 3, 6, 15, and 30, are shown. The discrimination task between stimuli at positions 3 and 6 is schematically illustrated with an asterisk. (*B*) Peri-stimulus time histogram (PSTH) at a long time scale (10-ms bin width, 100 repeats). Thick line below PSTH, duration of stimulus (50 ms) repeated once every second. (*C*) PSTH at a shorter time scale (1-ms bin width). Thick line, duration of stimulus; dashed line, time window for data analysis, 20–55 ms (see *Materials and Methods*). (*D*) Raster plot of responses of the 100 trials illustrated in *C* (1-ms bin width). (*E*) Spike-count distribution of the same 100 trials illustrated in *C*. Data analysis window for *C*–*E*: 20–55 ms.

response peak latency was used to estimate the diameter (width) of the RF center, which was taken as its width at 20% of maximum. The diameters ranged from 1.0 to 4.4° at eccentricities from 6.6 to 12.0°. Similar values were obtained with bar stimuli and white noise (maximum difference, 25%; average difference, 2.6%; $n = 14$). Both X cells ($n = 7$) and Y cells ($n = 7$) were included in this study. Classification was based on the width of the RF, compared with others at the same eccentricity, and on the temporal dynamics of the visual response (21).

During the experiments, vertical bars (100% contrast, black or white depending on whether the cell was on-center or off-center) were presented at multiple positions in the RF with spatial increments of 2.4–5.8% of the RF size of the cell (mean 3.8%) (see Fig. 1*A*). The length of the bar stimulus was 14.5° (29 cm at 114 cm from the eye) and the width varied between 0.17–1.81° (13- 41% of the RF diameter of the cell, mean 24%). Compared with the width of the RF center, the bars were fairly wide to evoke robust responses to brief flashes, but the spatial increments were very small. For each position, the vertical bar was presented every second for a duration of 50 ms. We chose to use such briefly flashed bars so that the stimulus presentation was similar to that used in psychophysical experiments (10, 11) under conditions for which stimulus motion is minimized. The psychophysical vernier acuity does not vary much when the stimulus is presented longer than this duration (24). To obtain the distributions of spike-count responses, the stimulus was repeated at least 100 times at each location.

Neuronal Response and Characterization. Responses to the 50-ms stimulus always started with a strong, transient response, sometimes followed by a second peak ≈100 ms later (Fig. 1*B*). In the analysis presented here, we consider only the spikes during the initial transient period (the first narrow peaks in Fig. 1*B*). This initial transient period was determined during examination of the more detailed peri-stimulus time histogram at 5-ms bins (dashed lines in Fig. 1*C*, 20–55 ms). In all cases, when the histogram was plotted with 5-ms bins, there was a well defined period with a continuous response, whose onset was in the range 0–50 ms and whose duration was <100 ms. For each cell, all further analysis was performed on spikes in what we term the ''initial transient period,'' determined from the stimulus position that evoked the longest initial response (as in Fig. 1*C*, position 6).

In all analyses, we assume that the neuronal information depends only on the number of spikes during this initial transient period, not on the relative timing of the spikes. To examine the ability of a neuron to discriminate based on the number of spikes evoked in single trials, we consider the distribution of spike counts (in all 100 trials) (Fig. 1*E*) and not just the average rate, providing a complete characterization of the responses to the bar stimulus at each position.

Data Analysis. The ability to make spatial discriminations was quantified by calculating the probability of making a correct two-alternative forced choice between two nearby stimuli. For each stimulus position i ($i = 1, 2, 3 \ldots$), we assumed that responses were characterized completely by the distribution of spike-counts $p_i(r)$, in which r represents the response from a single trial. We used a maximum likelihood procedure to calculate a two-alternative forced-choice between two stimuli (s_i and s_j). For each of the 100 trials, an individual test response (r_{test}) was compared with the two spike-count distributions: $p_i(r)$ and $p_j(r)$. When the two probabilities were different [$p_i(r_{\text{test}}) \neq p_j(r_{\text{test}})$], the stimulus position corresponding to the higher probability was chosen; when the probabilities from the two distributions were the same [$p_i(r_{\text{test}}) = p_j(r_{\text{test}})$], the chosen stimulus was randomly assigned between the two possibilities. To prevent a trial from being used to predict itself, each trial was compared with spike-count distributions calculated from the 99 other trials. The ability of the cell to discriminate two stimuli was evaluated as the percentage of correct neuronal choices in the 100 trials: the total number of correct decisions (for each of the two positions) divided by the total number of responses tested (200).

The calculation of our two-stage neuronal decision model (see Fig. 4) is based on following assumptions: (*i*) all pooled cells are identical; (*ii*) responses are statistically independent so the signal/noise ratio improves as the square root of number of cells; and (*iii*) the acuity threshold improves at the same rate as the signal/noise. The number of neurons selected for pooling (see Fig. 4*A*) is determined based on the coverage factor of 4 in cat area centralis (25). If the performance range is one-half RF, then ≈2 neurons are added as the bar length is increased by 1 RF width; if the performance range is one-quarter RF, ≈1 neuron is added for the same increase in length.

Results

To study the ability of single neurons to discriminate under conditions comparable with psychophysics, we recorded the responses of cat LGN cells to bar stimuli at very fine resolution throughout the entire RF. From left to right in the example shown in Fig. 1*A*, the bar stimulus was flashed at 33 positions (indicated by tick marks, spacing: 0.057°). The stimuli at positions 3, 6, 15, and 30 are illustrated, and the task for discriminating two nearby stimuli at position 3 and 6 is schematically shown. Responses to the 50-ms stimulus always started with a strong, transient response, sometimes followed by a second peak ≈100 ms later (Fig. 1*B*). In the analysis presented here, we consider only the responses during the initial transient period, the first peak in Fig. 1*B* (corresponding to 20–55 ms, indicated by the dashed line in Fig. 1 *C* and *D*, see *Materials and Methods*). Although a close examination of this initial transient response revealed some temporal structure (Fig. 1 *C* and *D*), we restricted our analysis to the number of spikes during this initial transient period, not on the relative timing of the spikes. With 100 repeats at each stimulus location, the neuronal information about the stimulus position was fully characterized as spike count distributions (Fig. 1*E*).

The fine spatial increment of the stimulus across the receptive field resulted in a gradual change in response magnitudes (Fig. 2 *A* and *B*). From left to right in Fig. 2*A*, the average spike rate (20–55 ms window, 100 repeats) increased gradually to its peak value at position 15, and it then declined slowly back to its minimal value at position 33 (Fig. 2*A*). This gradual change can also be observed by plotting separately the probability of each given spike-count response at all positions (Fig. 2*B*). For instance, the probability of having three spikes in a single trial was >50% for stimuli located at the center of the RF (Fig. 2*B*, stimulus position 11–14) but near 0% at the edge of the RF.

To translate these data into a neurometric measure of single-cell performance, we calculated how well the responses to stimuli at one location could be distinguished from the responses to stimuli at another location. Because the spike-count distributions from the two locations were known, we used a maximum likelihood procedure to make a choice from a single-trial response to a single-stimulus presentation. Given the two alternatives, the stimulus with higher probability of evoking the response was chosen. Performance was quantified as the percentage of trials for which the correct discrimination was made. In Fig. 2*C*, we illustrate the performance of our example cell across its receptive field by plotting "location discrimination curves." The *x* axis gives the midpoint of each pair of stimuli, and the *y* axis shows the percentage of correct neuronal choices. Each of the six curves corresponds to a fixed spacing between the two stimuli.

The location discrimination curves can be related to a psychophysical vernier task as follows. Assuming that there is an upper reference bar, collinear with one of the two stimuli presented to the cell, we measured the percentage of the time that the two lower stimuli evoke responses that can be correctly distinguished from each other. In general, the more distinct the two underlying response distributions (Fig. 2*B*), the greater the probability of a correct discrimination (Fig. 2*C*). Discrimination was better when the two stimuli were widely spaced (compare curves 1–6, spacing from 0.057 to 0.342°) and when they were centered around the position in the response curve that had the greatest slope (Fig. 2 *A* and *C*, large arrows). Discrimination approached chance levels when the two stimuli were centered around positions where the slope was near zero (Fig. 2 *A* and *C*, small arrows). Within a RF, the single-cell discrimination was finest at the position where responses were changing most rapidly but was poor at the center and edges of the RF.

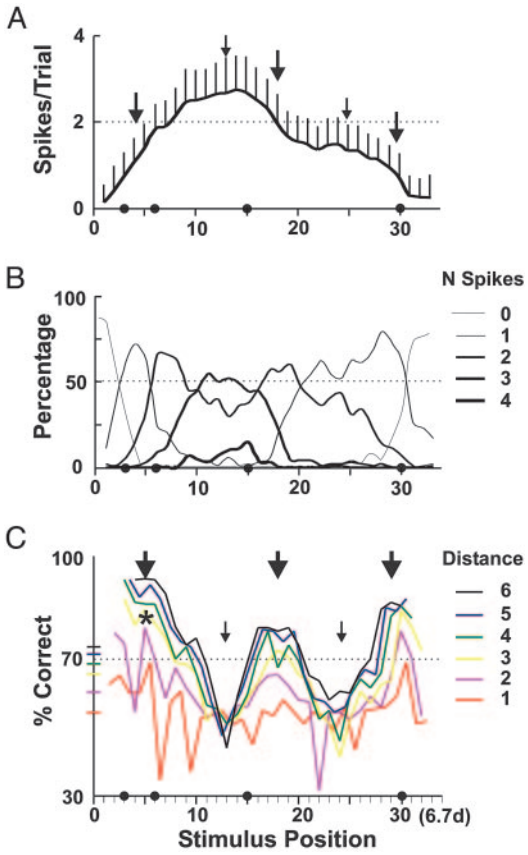

Fig. 2. Responses and discriminations at all positions across the receptive field. (*A*) Averaged firing rates (from 100 repeats) at 33 positions across the RF for the same LGN cell in Fig. 1. Error bars, 1 SD. Circles on abscissa indicate the positions 3, 6, 15, and 30 as illustrated in Fig. 1. (*B*) Spike-count distributions at all 33 positions. Lines in this graph show the percentage of trials that had a given number of spikes (0, 1, 2, 3, or 4). (*C*) Discrimination rates between two nearby stimuli centered at different positions in the RF, derived from the spike-count distributions by using a maximum likelihood procedure. Different lines correspond to different spacings between stimuli [from 1 (0.057°) to 6 (0.342°)]. Colored tick marks on the *y* axis correspond to the averaged discrimination rates over the entire RF. Large arrows, positions with fastest rate of change (*A*) and highest discrimination rates (*C*); small arrows, positions with slowest rate of change (*A*) and lowest discrimination rates (*C*). The asterisk in *C* indicates the discrimination rate between positions 3 and 6 (see Fig. 1*A*).

In psychophysics, vernier acuity is determined from performance curves, which plot the correct discrimination rate as a function of relative distance between two stimuli. In previous psychophysical work on cats, the vernier threshold has been defined as the distance between stimuli for which animals made a correct discrimination 70% of the time (13, 14). Vernier thresholds in cats have been found to be in the range of 1.2 (14) to 2.3 minutes of arc (hereafter, min arc) (13). To compare our single-cell results to psychophysical acuity values in cats, the psychophysical data were normalized by the smallest RFs that have been observed in physiological studies, 0.25° (25–28) (1.2 min arc = 0.02°, 8% of the RF width; 2.3 min arc = 0.04°, 15% RF).

Analogously, a performance curve for a single cell would give the probability that a discrimination could be made as a function of the distance between stimuli. Because the ability of a cell to perform a discrimination task depends on the position of stimuli within the RF (Fig. 2*C*), a single-cell performance curve depends on where the stimuli can fall. The simplest assumption is that the two stimuli are centered around the best position, the position

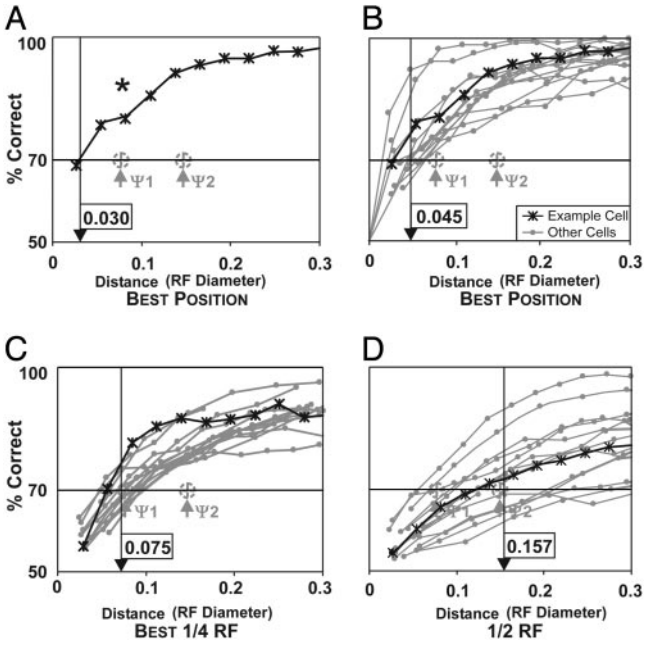

Fig. 3. Discrimination rates at best position, best one-quarter RF, and one-half RF. (*A*) Rate of discrimination between two stimuli as a function of interstimulus distance for the cell illustrated in Figs. 1 and 2, taken at the single position with best performance (Fig. 2, position 4). Abscissa (distance) is normalized by the diameter of the RF center (2.05°). Large arrow (0.030 RF), acuity threshold at 70% correct. Minimum interstimulus spacing, 0.028 RF. The asterisk indicates the discrimination rate between positions 3 and 6 (see Figs. 1 and 2*C*). Dashed circles ψ 1 (0.08 RF) and ψ 2 (0.15 RF), 70% minimal distinguishable distances derived from behavioral experiments (13, 14). (*B*) Single-cell discrimination rate at the best position for 14 LGN cells is better than behavioral results (asterisks indicate the cell illustrated in Figs. 1 and 2). Large arrow (0.045 RF), averaged single-cell acuity at 70% correct. (*C*) Averaged single-cell discrimination rate at the most sensitive quarter of RF is very close to behavioral results. Large arrow (0.075 RF), averaged acuity at 70% correct. (*D*) Averaged single-cell discrimination rate within one-half RF is worse than behavioral results. Large arrow (0.157 RF), averaged single-cell acuity at 70% correct.

with highest discrimination rates in the RF (Fig. 2*C*, thick arrow at left). In the example shown (Fig. 3*A*), 70% correct discrimination was achieved for two stimuli separated by only 0.06°, i.e., the acuity was 3% RF (RF diameter = 2.05°). For this cell at its best position, discrimination of two stimuli separated by 3% RF was far better than the best psychophysical acuity of 8% RF. In Fig. 3*B*, we plot performance curves of 14 cells at their most sensitive position. On average, the 70% threshold was for stimuli separated by 4.5% RF. Compared with the best measured acuity level (8% RF) from cat behavioral studies, the acuity threshold of single cells at their most sensitive locations was ≈2-fold superior.

Past studies have also reached the conclusion that single-cell performance is better than psychophysical performance, provided that stimuli are located at an optimal position in the RF (17, 18). The stimulus in a psychophysical task, however, cannot be assumed to fall within the most sensitive location in any given RF. One should therefore ask a more general question: What is the average performance of a single cell when the stimulus is allowed to fall within a specific range of locations, the ''performance range''? Given that a stimulus falls at a random position on the retinal ganglion cell mosaic, the specification of the performance range is equivalent to selecting a group of neurons that might participate in the discrimination task. One assumption is that the performance range is large enough to allow the stimuli to fall anywhere within the entire RF (or by symmetry, one-half of the RF). Under this condition, a single-cell performance curve would be equal to the average of the curves from all points in the RF (Fig. 3*D*). Because certain stimulus locations evoke less discriminable responses, single-cell performance averaged over the entire RF (Fig. 3*D*) is worse than performance at its best point (Fig. 3*B*). The acuity threshold of our example cell performing through its whole RF was 12.4% RF, whereas the threshold for the same cell performing at its most sensitive point was 3% RF (Figs. 3 *A*, *B*, and *D*). On average, if stimuli could fall anywhere within the cell's RF, then the vernier threshold of a single cell was 15.7% RF, two times worse than behavior (Fig. 3*D*).

Between the two extremes of the best position and the entire RF, the performance range could be any fraction of the RF. In Fig. 3*C*, we show the performance of a single cell when the stimuli were restricted to the best quarter of that cell's RF. In this case, the 70% acuity thresholds (4.8–9.7% RF widths; mean, 7.5%) were close to the finest measured psychophysical thresholds (Ψ 1 = 8% RF; refs. 13 and 14). Taken together, the results illustrated in Fig. 3 suggest that behavioral performance levels on a vernier task can be matched by the responses of a single cell only if the performance range is restricted to the most discriminating quarter of the RF (Fig. 3*C*).

More generally, one can ask how a vernier discrimination might be constructed based on the responses of an ensemble of LGN neurons. Here, we use the retinal ganglion cell mosaic, a first approximation of the mosaic of LGN neurons, as a framework to assess how neurons might participate in a vernier task. We propose a simple two-stage decision model for making a vernier judgment from the responses of neurons in a retinal ganglion cell mosaic. First, a group of neurons is selected based on their RF positions relative to the stimulus (the performance range, Fig. 4*A*). Second, a decision is reached by integrating the responses of the neurons selected (Fig. 4*B*).

At the first stage (Fig. 4*A*), all neurons that might participate in the vernier task are selected based on the performance range and the stimulus size and location. As would be expected, the greater the performance range and the longer the bar stimulus, the more neurons would be selected to participate in the discrimination task. From left to right, we illustrate the selection process for four performance ranges: the best point, the best one-quarter of RFs, the one-half of RFs, and the whole RF. Not all performance ranges are reasonable choices for studying vernier decision, however. If the performance range is the best position (Fig. 4*A i*), then we must assume that the first stage can perform with hyperacuity, which makes the second stage irrelevant. At the opposite extreme, if the performance range is the full width of the RF (Fig. 4*A iv*), then the first stage is of course very simple, but such indiscriminant summation of responses significantly degrades spatial information. When responses from neurons on both sides of a bar are summed together (Fig. 4*A iv*), the net changes in responses of neurons on one side cancel the changes on the opposite side, so the overall ability to discriminate decreases to chance levels.

Given the ensemble of neurons selected in the first stage, the second stage determines the form of integration: whether the decision is based on a single cell (randomly chosen from all candidates) or pooling (linear summation of the responses from all candidates). As noted above, we found that for a single neuron to reach the behavioral threshold (1.0 Th_{Behav} in Fig. 4 *B i*), the cell must be located such that the stimulus falls in the best quarter of its RF. Alternatively, if the response is determined by pooling multiple neurons (Fig. 4 *B ii*), then a similar level of vernier acuity can be achieved by summing a few cells (≈4) that are located on one side of the bar stimulus (one-half RF).

To further constrain the parameters in the model, we compared the theoretical behavior with the actual dependence of

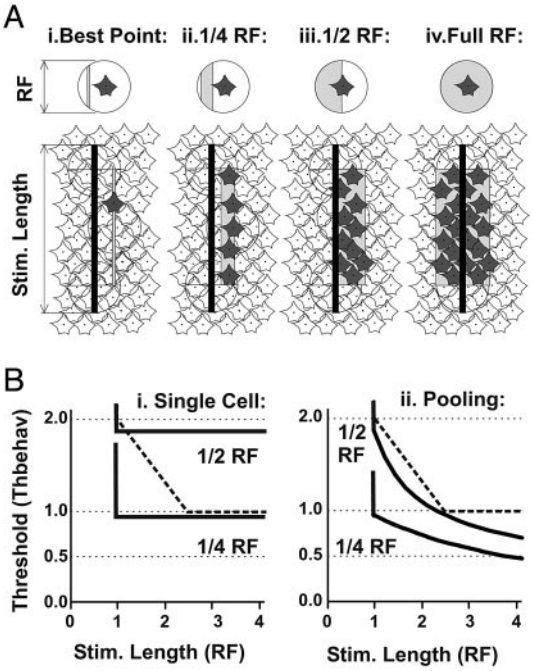

Fig. 4. Two-stage neuronal decision model: selection and integration. (*A*) The first stage is the selection of neurons involved, based on whether the stimulus is within a predetermined performance range for each RF. The wider the performance range or the longer the bar stimulus, the more neurons are selected. Performance ranges from left to right: best point, best one-quarter RF, best one-half RF, and full RF. (*Upper*) retinal ganglion cells and their RF centers (circles). Shaded areas, the performance range of individual neurons. (*Lower*) visual stimulus (bars) and cells that fulfill the selection criteria (shaded). Neurons are evenly distributed across the retina assuming a coverage factor of 4 (linear coverage factor = 2.10) (25). (*B*) The second stage is the integration of responses from selected neurons, illustrating how the acuity threshold is affected by using a single-cell acuity vs. pooling. Dark lines are for neurometric vernier thresholds based on different neuronal decision mechanisms. Thick dashed line are human psychometric vernier thresholds (11), assuming that the smallest RFs are ≈2 min arc (29–31). (*Left*) Single-cell, the decision is made from the response of one of the cells selected in *A*. Vernier thresholds therefore stay constant as the bar length is increased. (*Right*) Pooling, the decision is made from the pooled responses of all selected neurons in *A*. As the visual stimulus grows longer (more and more neurons are pooled), the vernier threshold declines as the square root of the total number of selected cells (see *Materials and Methods*).

vernier thresholds on stimulus length as measured psychophysically (11). Psychophysical vernier thresholds are elevated by approximately a factor of 2 when essentially point-like stimuli are used (≈2 min arc = 0.03° in length, equivalent to the smallest RFs reported from macaques) (29–31). As bar length increases, performance improves and then asymptotes at ≈5 min of arc (11). Within the framework of our model, this behavior (Fig. 4*B*, dashed lines) is best matched by summing the response from a few (up to four) neighboring cells located on one side of the bar stimulus.

Discussion

We have examined the question of how a decision on a vernier task might be constructed from the responses of individual neurons in a retinotopic mosaic. The responses of LGN neurons to closely spaced bars were recorded, and their ability to discriminate between them was calculated. At the positions within a RF where responses were changing most rapidly, the ability of a single cell to discriminate exceeded previously reported vernier acuity (13, 14). In the center and near the edges of the RF, where responses changed slowly, the ability of a single cell to discriminate was considerably worse than behavioral performance.

The demonstration that the regions of the receptive field with the greatest slope are most sensitive for vernier task is consistent with other studies. As shown in motion-discrimination tasks, the visual system relies on neurons that show intermediate responses to a given stimulus, rather than the neurons that are responding the strongest (32–35). Our estimations of a single cell's ability to discriminate at its most sensitive RF region is similar to those derived from other single-cell physiological studies (17–19). Under conditions comparable with behavioral experiments, in which all regions of the receptive field are equally likely to contribute to the discrimination, we found that the ability of a single cell to make a vernier discrimination is about two times worse than psychophysical acuity. This finding is one of the very rare cases in which the neuronal decision cannot be accounted for by the responses of single cells; the decision must be based on information integrated from more than one neuron (19).

Theoretically, there are many different ways to integrate the responses of multiple neurons to construct a neuronal decision. One of them is to make the decision based on the response of a single cell, preselected by the population response pattern where the stimulus falls in its most sensitive region (Fig. 2). Another one, pooling, is to make the decision based on the summed response of multiple neurons. To examine these two strategies on an equal footing, we proposed a two-stage model: selection followed by integration. Based on previously reported values of the retinal mosaic and the RF size of LGN neurons, we simulated the model and asked how a vernier discrimination could be accounted for by the responses of an ensemble within the retinotopic mosaic. To account for the psychophysical level of vernier acuity, the decision can be based either on the response of a single cell where the stimuli fall within its best quarter RF or the summed responses of about four neurons, all located on one side of the stimulus. In cats, simple cells receive input from a limited number of thalamic neurons clustered in an elongated region that is 2–3 times longer than an LGN receptive-field center (36). As has been suggested in refs. 18 and 37, simple cells are therefore likely the first candidates for the modest level of integration that best explains psychophysical vernier acuity.

We based our calculations on the maximum likelihood procedure because it directly translates a single-trial neuronal response into a single-trial two-alternative, forced-choice decision. However, this procedure gave very similar results (within 10–20%; analysis not shown) to those obtained with a simpler two-response comparison implemented as follows. We considered all pairings of the responses evoked by 100 repetitions of the stimulus at two different positions. When the two responses were equal, the stimulus corresponding to each was assigned with equal probability. For paired responses with different spike counts, the larger response was assigned to the stimulus closer to the RF center. A more standard receiver operating characteristic analysis (19) also gave results similar to our maximum likelihood procedure. The acuity level derived from the neuronal responses does therefore not strongly depend on the form of the data analysis performed. The similarity of the results from all three calculations suggests that the decision process can be as simple as taking the difference of two signals.

It is worth emphasizing that the ability to discriminate between stimuli at two positions is determined by the difference in the responses they evoke. This notion explains our single-cell result that the discrimination is finest at the region of highest slope but is poor at the center and edges of the RF (Fig. 2). Similar reasoning can also explain our pooling results: the ability to discriminate could be improved only by pooling additional neurons on the same side of the stimulus. When the responses of two neurons on the same side of the stimulus are pooled, the response changes are always in the same direction. The overall

ability to discriminate can be improved because the overall difference between the responses evoked by different stimuli is enlarged, i.e., the slope is steeper. However, when two neurons on the opposite side are pooled, the response changes are always on the opposite direction. The overall ability to discriminate is reduced because the two signals on the opposite direction cancel each other out.

More generally, this notion that the response difference determines discrimination can be extended to the decision process of other discrimination tasks. Assuming the discrimination is to distinguish stimulus A from stimulus B, the stimulus differences can be encoded by different neurons with either a response increment or decrement. Therefore, pooling the additional neurons with the same slope can improve the overall sensitivity while pooling neurons with opposite slopes degrades the overall sensitivity. In addition to adding noise, this result is another way in which the overall discrimination sensitivity can be degraded by pooling multiple neurons (38).

The idea that selectively combining (grouping) the responses of neurons with similar properties may play an important role in improving the overall sensitivity has been implied by anatomical, physiological, and behavioral experiments. Considering horizontal connections, it has been shown that they are clustered and involve cells and columns with like orientation and ocular dominant specificity (39–43). Combination of physiology and behavioral studies has shown that the visual system selectively relies on the neurons with intermediate responses during discrimination task instead of those with peak responses (32–35). Because the simple model we proposed here explicitly separates the neuronal decision process into selection followed by integration, it can serve as a framework for examining the relationship between selective grouping and the overall sensitivity. As such, it might further our understanding of how the overall discrimination might be improved by combining the responses of neurons with similar properties.

We thank Prakash Kara, John Assad, and Richard Born for critical reading of an earlier version of the manuscript; Peter Schiller for critical reading of a later version of the manuscript; and Carrie McAdams for making many helpful suggestions. This work was supported with National Institutes of Health (National Eye Institute R01 EY10115, R01 EY12815, and P30 EY12196).

1. Parker, A. J. & Newsome, W. T. (1998) *Ann. Rev. Neurosci.* **21,** 227–277.
2. Barlow, H. B. & Levick, W. R. (1969) *J. Physiol.* **200,** 1–24.
3. Talbot, W. H., Darian-Smith, I., Kornhuber, H. H. & Mountcastle, V. B. (1968) *J. Neurophysiol.* **31,** 301–334.
4. Vogels, R. & Orban, G. A. (1990) *J. Neurosci.* **10,** 3543–3558.
5. Tolhurst, D. J., Movshon, J. A. & Dean, A. M. (1983) *Vision Res.* **23,** 775–785.
6. Relkin, E. M. & Pelli, D. G. (1987) *J. Acoust. Soc. Am.* **82,** 1679–1691.
7. Hawken, M. J. & Parker, A. J. (1990) *In Vision: Coding and Efficiency*, ed. Blakemore, C. (Cambridge Univ. Press, Cambridge), pp. 103–116.
8. Barlow, H. B. (1995). in *The Cognitive Neuroscience*, ed. Gazzaniga, M. (MIT Press, Cambridge, MA), pp. 415–435.
9. Darian-Smith, I., Johnson, K. O. & Dykes, R. (1973) *J. Neurophysiol.* **36,** 325–346.
10. Westheimer, G. & Hauske, G. (1975) *Vision Res.* **15,** 1137–1141.
11. Westheimer, G. & McKee, S. P. (1977) *Vision Res.* **17,** 941–947.
12. Curcio, C. A. Sloan, K. R., Kalina, R. E. & Hendrickson, A. E. (1990) *J. Comp. Neurol.* **292,** 497–523.
13. Belleville, S. & Wilkinson, F. (1986) *Vision Res.* **26,** 1263–1271.
14. Murphy, K. M. & Mitchell, D. E. (1991) *Vision Res.* **31,** 253–266.
15. Kiorpes, L., Kiper, D. C. & Movshon, J. A. (1993) *Vision Res.* **33,** 2301–2311.
16. Kiorpes, L. (1992) *Vis. Neurosci.* **9,** 243–251.
17. Shapley, R. & Victor, J. (1986) *Science* **231,** 999–1002.
18. Parker, A. & Hawken, M. (1985) *J. Opt. Soc. Am. A* **2,** 1101–1114.
19. Lee, B. B., Wehrhahn, C., Westheimer, G. & Kremers, J. (*1993*) *J. Neurosci.* **13,** 1001–1009.
20. Usrey, W. M., Reppas, J. B. & Reid, R. C. (1999) *J. Neurophysiol.* **82,** 3527–3540.
21. Alonso, J. M., Usrey, W. M. & Reid, R. C. (2001) *J. Neurosci.* **21,** 4002–4015.
22. Reid, R. C., Victor, J. D. & Shapley, R. M. (1997) *Vis. Neurosci.* **14,** 1015–1027.
23. Jones, J. P. & Palmer, L. A. (1987) *J. Neurophysiol.* **58,** 1187–1211.
24. Waugh, S. J. & Levi, D. M. (2000) *Vision Res.* **40,** 163–171.
25. Peichl, L. & Wässle, H. (1979) *J. Physiol. (London)* **291,** 117–141.
26. Cleland, B. G., Harding, T. H. & Tulunay-Keesey, U. (1979) *Science* **205,** 1015–1017.
27. Cleland, B. G. & Levick, W. R. (1974) *J. Physiol. (London)* **240,** 421–456.
28. Linsenmeier, R. A., Frishman, L. J., Jakiela, H. G. & Enroth-Cugell, C. (1982) *Vision Res.* **22,** 1173–1183.
29. Hubel, D. H. & Wiesel, T. N. (1966) *Proc. Natl. Acad. Sci. USA* **55,** 1345–1346.
30. De Monasterio, F. M. & Gouras, P. (1975) *J. Physiol. (London)* **251,** 167–195.
31. Poggio, G. F., Doty, R. W. Jr., & Talbot, W. H. (1977) *J. Neurophysiol.* **40,** 1369–1391.
32. Regan, D. & Beverley, K. I. (1983) *J. Opt. Soc. Am.* **73,** 1684–1690.
33. Regan, D. & Beverley, K. I. (1985) *J. Opt. Soc. Am. A* **2,** 147–155.
34. Treue, S., Hol, K. & Rauber, H. J. (2000) *Nat. Neurosci.* **3,** 270–276.
35. Hol, K. & Treue, S. (2001) *Vis. Res.* **41,** 685–689.
36. Reid, R. C. & Alonso, J. M. (1995) *Nature* **378,** 281–284.
37. Swindale, N. V. & Cynader, M. S. (1986) *Nature* **319,** 591–593.
38. Shadlen, M. N. & Newsome, W. T. (1995) *Curr. Opin. Neurobiol.* **5,** 248–250.
39. Gilbert, C. D. & Wiesel, T. N. (1983) *J. Neurosci.* **3,** 1116–1133.
40. Ts'o, D. Y., Gilbert, C. D. & Wiesel, T. N. (1986) *J. Neurosci.* **6,** 1160–1170.
41. Rockland, K. S. & Lund, J. S. (1982) *Science* **215,** 1532–1534.
42. Bosking, W. H., Zhang, Y., Schofield, B. & Fitzpatrick, D. (1997) *J. Neurosci.* **17,** 2112–2127.
43. Chisum, H. J. & Fitzpatrick, D. (2004) *Neural Netw.* **17,** 681–693.